



# Effectiveness of feedback control and the trade-off between death by COVID-19 and costs of countermeasures

Akira Watanabe<sup>1</sup> · Hiroyuki Matsuda<sup>1</sup>

Received: 14 April 2021 / Accepted: 15 September 2022

© The Author(s), under exclusive licence to Springer Science+Business Media, LLC, part of Springer Nature 2022

## Abstract

We provided a framework of a mathematical epidemic modeling and a countermeasure against the novel coronavirus disease (COVID-19) under no vaccines and specific medicines. The fact that even asymptomatic cases are infectious plays an important role for disease transmission and control. Some patients recover without developing the disease; therefore, the actual number of infected persons is expected to be greater than the number of confirmed cases of infection. Our study distinguished between cases of confirmed infection and infected persons in public places to investigate the effect of isolation. An epidemic model was established by utilizing a modified extended Susceptible-Exposed-Infectious-Recovered model incorporating three types of infectious and isolated compartments, abbreviated as SEIIHHHR. Assuming that the intensity of behavioral restrictions can be controlled and be divided into multiple levels, we proposed the feedback controller approach to implement behavioral restrictions based on the active number of hospitalized persons. Numerical simulations were conducted using different detection rates and symptomatic ratios of infected persons. We investigated the appropriate timing for changing the degree of behavioral restrictions and confirmed that early initiating behavioral restrictions is a reasonable measure to reduce the burden on the health care system. We also examined the trade-off between reducing the cumulative number of deaths by the COVID-19 and saving the cost to prevent the spread of the virus. We concluded that a bang-bang control of the behavioral restriction can reduce the socio-economic cost, while a control of the restrictions with multiple levels can reduce the cumulative number of deaths by infection.

**Keywords** Non-pharmaceutical intervention · Feedback control · Epidemic model · Isolation of asymptotically infected persons · Optimal control

## Highlights

- Our study distinguished between cases of confirmed infection and infected persons in public places to investigate the effect of isolation.
- A feedback controller approach based on the active number of hospitalized persons is proposed to reduce the damage from the novel coronavirus.
- Early initiating behavioral restrictions is a reasonable measure to reduce the burden on the health care system.
- A bang-bang control of the behavioral restriction can reduce the socio-economic cost, while a control of the restrictions with multiple levels can reduce the cumulative number of deaths by infection.

## 1 Introduction

The number of novel coronavirus (COVID-19) cases, caused by severe acute respiratory syndrome coronavirus 2 (SARS-CoV-2), has been increasing worldwide since late 2019. The actual numbers of infected persons, isolated persons, and infection-related deaths depend on the effective reproduction number, which is defined as the average number of people infected by an infectious person by the time of his or her recovery. Reducing the reproduction number is necessary to suppress this epidemic. Previous studies have shown that this can be achieved by reducing three factors, namely: the susceptibility of uninfected persons, contact rates in the population, or the infectiousness of infected persons [15].

Regarding measures against infectious diseases undertaken by policymakers, two fundamental strategies exist: suppression and mitigation [17]. The suppression strategy involves reducing the number of cases to a low level and is used in diseases with high mortality rates and low infection rates. In contrast, mitigation strategies involve slowing and reducing the peak of

✉ Akira Watanabe  
akirawatanabe.acdmy1@gmail.com

Hiroyuki Matsuda  
hymatsuda@gmail.com

<sup>1</sup> Graduate School of Environment and Information Sciences,  
Yokohama National University, Yokohama, Japan

infections and are used in diseases with low mortality rates and high infection rates. The vaccine against the COVID-19 has been developed and released by some medicine companies since the outbreak. However, in the present study, we focus on the period without the aid of vaccines or specific medicines and reducing contact rates in the population by conducting non-pharmaceutical interventions. Anti-contagion policies and measures have been discussed in some countries, and their effects, estimated, (e.g., [11, 15, 16, 24]). The Japanese government undertook several countermeasures, such as declaring a state of emergency, implementing priority preventive measures, and urging people to avoid the “Three Cs,” which refer to closed spaces, crowded places, and close-contact settings [8, 34].

The data obtained from observational research has revealed the features of the SARS-CoV-2 infection [22, 42–44, 64]. Nishiura et al. [43] reported that the serial interval of SARS-CoV-2 infection is close to or shorter than its median incubation period. This implies that transmission may occur before the onset of clinical symptoms or during asymptomatic infection. Such transmission may reduce the effectiveness of simple public measures, such as isolating symptomatic persons and tracing and quarantining their contacts [18]. In addition, it is important to estimate the exact number of infected persons in order to appropriately implement public health policies. Some studies assessed cases of unobserved infection and argued that the pandemic had been more broadly spread than the number of confirmed cases (e.g., [6, 7, 52, 63]).

Many researchers have proposed new epidemic models to describe the behavior of the novel coronavirus, extending and modifying the Susceptible-Infectious-Recovered (SIR) or Susceptible-Exposed-Infectious-Recovered (SEIR) models. The epidemic model was established to design a strategy for managing the pandemic and studying the impact of non-pharmaceutical interventions, such as lockdown [14, 47], testing [48], contact tracing, and isolation [23]. Senapati et al. [54] revealed that greater intervention effort is required to control the disease outbreak within a shorter period of time. Wood et al. [65] investigated the effectiveness of increasing healthcare capacity and extending the period of isolation. Some studies distinguish between and incorporate both asymptomatic and symptomatic persons, who play an important role in the COVID-19 pandemic (e.g., [3, 9, 19, 20, 25, 29, 40, 54, 62]). Moreover, the infectiousness of asymptomatic infected cases has been reported to be lower than that of symptomatically infected cases [22, 39]. Gevertz et al. [19], Kuniya and Inaba [29], and Senapati et al. [54] incorporated the differences into their epidemic models.

The increase in detection and isolation of asymptotically infected persons appears to be effective as susceptible persons are prevented from being exposed to the virus from infected persons, including those that are asymptomatic. We divided the non-pharmaceutical interventions into two parts, namely: 1) the detection and isolation of asymptotically infected persons and 2) behavioral restrictions, such as

requesting restricted business hours and physical distancing. Some researchers use “social” distancing; however, we use “physical” distancing to emphasize in-person contact.

There is a trade-off between the negative impact on the economy and the reduction of infection-related deaths as a result of behavioral restrictions. Implementing behavioral restrictions contributes to reducing the reproduction number and preventing the spread of the virus; however, intense and prolonged restrictions decrease economic activities. To balance preventing the epidemic and maintaining economic activities is important for policymakers [9, 26, 30, 58]. Thunström et al. [58] conducted a benefit cost analysis of physical distancing measure to control the COVID-19 outbreak. Lasaulce et al. [30] found the optimal trade-off between economic and health impact by solving the optimization problem confined to the number of Intensive Care Units patients with the SEIR model given the duration of interest for the epidemic is six months. Accordingly, we prepared the following indicators: the cumulative number of deaths by COVID-19, the socio-economic cost caused by the behavioral restrictions, the total number of isolated patients, and the total number of tests taken to detect infected persons.

This paper aims to reduce the damage caused by COVID-19 and provide some insights into the pandemic by utilizing mathematical modeling, taking Tokyo, Japan as an example. We recommend a feedback controller approach to decide the degree of behavioral restrictions to be undertaken during the epidemic management period, which policymakers can adjust based on observational data. The feedback control system is expected to be a robust and effective means against uncertainty. Dias et al. [13] proposed a control law of physical distancing within the SIR model, using the number of hospitalized persons as the feedback signal. Furthermore, during an epidemic, it is necessary to determine the proper timing during which to take preventive measures as well as establish the appropriate degree of behavioral restrictions. Di Lauro et al. [12] investigated the optimal timing of a one-time intervention using three indices, as follows: impact on attack rate, peak prevalence, and timing of infections. We conducted simulations of the feedback control of the degree of behavioral restrictions and demonstrated its effect and the timing at which to reduce the indicators by adjusting it. We also investigated the effects of detecting and isolating asymptotically infected persons.

## 2 Methods

### 2.1 Model

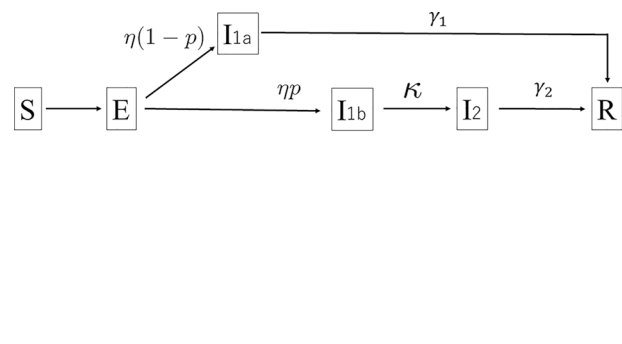
Our basic model is the SEIIR model, which is a modified version of the model that Kuniya and Inaba [29] proposed as an extended SEIR model. The infection spreads through asymptomatic and symptomatic persons. We assume that some infected persons recover without developing any symptoms,

while others develop them later on in the course of their infection. Hereafter, the former and latter are described as asymptomatic and presymptomatically infected persons, respectively.

$$\begin{cases} \frac{dS}{dt} = -(\beta_1(I_{1a} + I_{1b}) + \beta_2 I_2) \frac{S}{N} \\ \frac{dE}{dt} = (\beta_1(I_{1a} + I_{1b}) + \beta_2 I_2) \frac{S}{N} - \eta E \\ \frac{dI_{1a}}{dt} = \eta(1-p)E - \gamma_1 I_{1a} \\ \frac{dI_{1b}}{dt} = \eta p E - \kappa I_{1b} \\ \frac{dI_2}{dt} = \kappa I_{1b} - \gamma_2 I_2 \\ \frac{dR}{dt} = \gamma_1 I_{1a} + \gamma_2 I_2 \end{cases} \quad (1)$$

where  $S, E, I_{1a}, I_{1b}, I_2,$  and  $R$  represent the number of susceptible, exposed, asymptomatic, presymptomatically infected, symptomatically infected, and recovered persons, respectively.  $N$  is the total population size, including the number of deaths.  $N = S(t) + E(t) + I_{1a}(t) + I_{1b}(t) + I_2(t) + R(t)$ .  $\beta_1$  is the transmission rate of asymptomatic persons, while  $\beta_2$  is that of symptomatically infected persons.  $\gamma_1$  is the recovery rate of asymptomatic persons, while  $\gamma_2$  is that of symptomatically infected persons.  $\eta$  is the reciprocal of the latent period.  $\kappa$  is the reciprocal of the difference between the incubation period and the latent period.  $p$  is the proportion of infected persons who develop symptoms. In other words,  $1 - p$  refers to those who were infected and recovered without the onset of any symptoms. Note that those who are infected but do not have any symptoms are divided into  $I_{1a}$  and  $I_{1b}$ , but they cannot be distinguished by appearance. Figure 1(a) shows a schematic diagram of Eq. 1. The basic reproduction number  $\mathfrak{R}_0$  is as follows (see Appendix A for the derivation):

$$\mathfrak{R}_0 = (1-p) \frac{\beta_1}{\gamma_1} + p \frac{\beta_1}{\kappa} + p \frac{\beta_2}{\gamma_2} \quad (2)$$



(a) The SEIIR model: no isolation  $\theta = 0$  and  $H_c(t) = 0$

$I_{1a}, I_{1b},$  and  $I_2$  are not isolated and have the opportunity to infect susceptible persons. Let

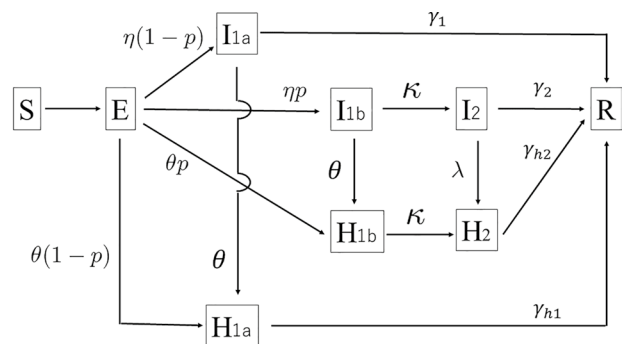
$$\mathfrak{R}_{01} = (1-p) \frac{\beta_1}{\gamma_1} + p \frac{\beta_1}{\kappa}, \text{ and } \mathfrak{R}_{02} = p \frac{\beta_2}{\gamma_2} \quad (3)$$

are the reproduction numbers for the asymptomatic and symptomatic infection, respectively. Note that  $\mathfrak{R}_0 = \mathfrak{R}_{01} + \mathfrak{R}_{02}$ . According to He, X. et al. [22], 44 percent of infection cases arise from the asymptomatic infection. Thus, in our context, we assume  $\mathfrak{R}_{01} = 0.44\mathfrak{R}_0$  and  $\mathfrak{R}_{02} = 0.56\mathfrak{R}_0$ .  $\beta_1$  and  $\beta_2$  are calculated using Eq. 2 and these equations.

$$\beta_1 = \frac{0.44\mathfrak{R}_0\gamma_1\kappa}{(1-p)\kappa + p\gamma_1}, \text{ and } \beta_2 = \frac{0.56\mathfrak{R}_0\gamma_2}{p} \quad (4)$$

The SEIIR model is modified and extended into the SEIIHHHR model by incorporating three different compartments for isolation:  $H_{1a}, H_{1b},$  and  $H_2$ .

$$\begin{cases} \frac{dS}{dt} = -(1-f)(\beta_1(I_{1a} + I_{1b}) + \beta_2 I_2) \frac{S}{N} \\ \frac{dE}{dt} = (1-f)(\beta_1(I_{1a} + I_{1b}) + \beta_2 I_2) \frac{S}{N} - \eta E - \theta E \\ \frac{dI_{1a}}{dt} = \eta(1-p)E - \gamma_1 I_{1a} - \theta I_{1a} \\ \frac{dI_{1b}}{dt} = \eta p E - \kappa I_{1b} - \theta I_{1b} \\ \frac{dI_2}{dt} = \kappa I_{1b} - \gamma_2 I_2 - \lambda I_2 \\ \frac{dH_{1a}}{dt} = \theta(1-p)E + \theta I_{1a} - \gamma_{h1} H_{1a} \\ \frac{dH_{1b}}{dt} = \theta p E + \theta I_{1b} - \kappa H_{1b} \\ \frac{dH_2}{dt} = \lambda I_2 + \kappa H_{1b} - \gamma_{h2} H_2 \\ \frac{dR}{dt} = \gamma_1 I_{1a} + \gamma_2 I_2 + \gamma_{h1} H_{1a} + \gamma_{h2} H_2 \end{cases} \quad (5)$$



(b) The SEIIHHHR model:  $\theta \geq 0$  and  $H_c(t) > 0$

Fig. 1 The epidemic model

where  $H_{1a}$ ,  $H_{1b}$ , and  $H_2$  represent the number of isolated asymptomatic, isolated presymptomatically infected, and isolated symptomatically infected persons, respectively. A schematic of Eq. 5 is shown in Fig. 1(b). The total population  $N = S(t) + E(t) + I_{1a}(t) + I_{1b}(t) + I_2(t) + H_{1a}(t) + H_{1b}(t) + H_2(t) + R(t)$  is constant for any time  $t$ ;  $f$  is the degree of the behavioral restrictions. While  $f = 0$  represents the absence of behavioral restrictions,  $f > 0$  means that some policies, such as restriction of movement, are implemented.  $\lambda$  is the reciprocal of the time from onset to isolation. The parameter  $\gamma$  denotes the recovery rate. The reciprocals of  $\gamma_2$  and  $\gamma_{h1}$  are the mean time periods from symptom onset to recovery and the average isolation period for those who are isolated at home or in hotels, respectively. People in compartment  $H_{1a}$  recover without the onset of symptoms, whereas people in  $H_{1b}$  develop some symptoms and are transferred to  $H_2$ . Note that those in  $H_{1a}$  and  $H_{1b}$  cannot be distinguished in terms of appearance. The transition from compartment  $H_{1b}$  to  $H_2$  means that an infected person is detected as a positive case and develops some symptoms later. The transition rate is assumed to be the same as  $\kappa$ . In this study, we assume that isolated persons without any symptoms stay at home or in hotels and do not occupy beds in hospitals or other healthcare facilities. The compartment  $R$  includes death. Note that for simplicity, the loss of immunity is ignored in this model within the management period.

It is assumed that those who get sick die of infection at a rate. Let  $D(t)$  be the number of deaths by COVID-19 in those who are newly confirmed cases from time 0 to  $t$ . we calculate it as follows:

$$D(t) = \delta \times \int_0^t (\theta(E(u) + I_{1a}(u) + I_{1b}(u)) + \kappa I_{1b}(u)) du \quad (6)$$

where  $\delta$  is the case fatality rate, defined as the ratio of deaths to the number of confirmed infected persons. There is a time lag between infection and recovery or death, but the difference is negligible.

## 2.2 Feedback control of behavioral restrictions

This study explored the effectiveness of the feedback control of behavioral restrictions. The degree of behavioral restrictions  $f = f(t)$  is changed based on the number of isolated symptomatically infected persons  $H_2(t)$  and its trend of increasing or decreasing  $\dot{H}_2(t)$ . Pataro et al. [50] introduced a framework for optimizing the required levels of public health policies and referred to the importance of finely tuning the level of restriction on the population's mobility. In this study, we assume that the intensity of the intervention, such as behavioral restrictions, can be divided into, at most, four levels. Hereafter, the feedback control which has  $J$  levels of behavioral restrictions is referred to as “ $J$ -level.” We define  $f_1$  as the mean degree of behavioral restrictions under the emergency state, which was

executed in Tokyo from April 7 to May 25, 2020. In our simulation, let  $f_1 = 0.6$  from the utilization ratio of major stations in the capital area [38]. We assume that the  $J$ -level has  $J + 1$  situations and  $f(t)$  is discretely changed:  $0, f_1/J, 2 \times f_1/J, \dots, (J - 1) \times f_1/J$ , and  $f_1$ . For example, the 1-level uses only two different situations: an emergency situation ( $f(t) = f_1$ ) and its release ( $f(t) = 0$ ), whereas the 4-level uses  $f(t) = 0, f_1/4, 2 \times f_1/4, 3 \times f_1/4$ , and  $f_1$ . The 1-level means the “bang-bang control” on the analogy of the control theory. The feedback control with  $J > 1$  is collectively denoted by “multilevel.” Examples of dynamics of  $H_2(t)$  and  $f(t)$  different levels of feedback control are demonstrated in the [Supplementary file](#). To mimic the actual transition, the maximum behavioral restriction is initially implemented. In the multilevel feedback algorithm,  $\Delta f$ , which is the increment and decrement of the degree of behavioral restrictions, is narrowed when  $f(t)$  is changed to execute the appropriate degree, while  $\Delta f$  is constant in the algorithm of the 1-level. For example, if the 4-level is adopted,  $\Delta f$  is 0.6 at first and changes to  $\Delta f = 0.3, 0.15, 0.15$ , and  $\dots$ . The transition of  $\Delta f$  with different levels of feedback control is demonstrated in the [Supplementary file](#).

Loewenthal et al. [33] argued that it is important to shorten the response time for initiating physical distancing, rather than extending the period of lockdown. We introduce  $T_1$  and  $T_2$  as the response and execution times, respectively.  $T_1$  is the period from the time when  $H_2(t)$  reaches a criterion and  $\dot{H}_2(t) \neq 0$  to the time when  $f(t)$  is raised or lifted. We assume that  $T_1 = 7$  days is a valid response time for administrative services in terms of feasibility and changeability.  $T_2$  is the period from initiating the change in  $f(t)$  to restarting the monitoring of  $H_2(t)$ . We assume that  $T_2 = 14$  days is a valid execution time.

$H_c(t)$  refers to the capacity of healthcare facilities or the number of beds for infected persons who can receive sufficient healthcare treatment. We also introduce two thresholds  $G_{up}$  and  $G_{down}$  as parameters determined by policymakers, and they satisfy  $0 < G_{up} \leq 1$  and  $0 < G_{down} \leq 1$ . Decreasing  $G_{up}$  lowers the thresholds to raise the degree of behavioral restrictions  $f(t)$  and prevents  $H_2(t)$  from exceeding  $H_c(t)$ . In contrast, increasing  $G_{down}$  loosens the criteria to lower  $f(t)$  and shortens their duration. Hereafter, we define  $c_r(t)$  as the ratio of  $H_2(t)$  to  $H_c(t)$ , and let

$$c_r(t) = \frac{H_2(t)}{H_c(t)} \quad (7)$$

Then the condition that the behavioral restriction changes depends on  $c_r(t)$ . This  $c_r(t)$  means the occupied rate of healthcare facilities at time  $t$ . If  $c_r(t) > 1$ , the capacity of healthcare facilities is overwhelmed. When  $c_r(t)$  exceeds  $G_{up}$  and  $\dot{H}_2(t) > 0$ , the state of emergency is initiated  $T_1$  days later, and  $f(t) = f_1$ . The state continues  $T_2$  days after initiation, and then  $f(t)$  is lifted if  $c_r(t)$  falls below  $G_{down}$  and

**Table 1** The list of variables, indicators, and parameters

Symbol	Definition
$S(t)$	Number of susceptible persons at time $t$
$E(t)$	Number of those who are exposed to the virus at time $t$
$I_{1a}(t)$	Number of asymptotically infected persons (without being isolated) at time $t$
$I_{1b}(t)$	Number of presymptomatically infected persons (without being isolated) at time $t$
$I_2(t)$	Number of symptomatically infected persons (without being isolated) at time $t$
$R(t)$	Number of recovered persons at time $t$
$H_{1a}(t)$	Number of isolated persons without any symptoms at time $t$
$H_{1b}(t)$	Number of isolated presymptomatic persons at time $t$
$H_2(t)$	Number of isolated symptomatic persons at time $t$
$D(t)$	Number of those who are isolated into some health care facilities from time 0 to $t$ and die from infection
$f(t)$	Degree of behavioral restrictions, such as the restriction of movement and shortening business hours at time $t$
$C_f$	Socio-economic cost caused by the behavioral restrictions
$C_1$	Total number of isolated persons at home or in hotels
$C_2$	Total number of hospitalized persons
$C_D$	Total number of those who take the test to detect infected persons
$c_r(t)$	Occupied rate of health care facilities at time $t$ , defined as $H_2(t)/H_c$
$C_{r,max}$	The maximum occupied rate in the management period, defined as $\max c_r(t)$
$c_N$	Number of days in which the occupied rate of health care facilities is over 1
$G_{up}$	Coefficient to increase the degree of behavioral restrictions
$G_{down}$	Coefficient to decrease the degree of behavioral restrictions

$\dot{H}_2(t) < 0$ . Then,  $f(t)$  is raised or lifted discretely in response to  $c_r(t)$  and  $\dot{H}_2(t)$ . The detailed algorithm of feedback control is described in Appendix B.

### 2.3 Calculation of indicators

In 2020 (fiscal year), the Tokyo prefectural government budgeted about two trillion JPY for the measure against the novel coronavirus. The budget included four purposes: 1) to prevent the spread of the virus (1,174 billion JPY), 2) to reinforce a safety net to support economic activities and civic life (990 billion JPY), 3) to balance the prevention of spreading the virus and economic activities (20 billion JPY), and 4) to reform the social structure to adapt to the epidemic (55 billion JPY) [61]. The basis for calculation is not so clear, and the use is various. Thus, we established the following five indicators which seem essentially important: the cumulative number of infected deaths by COVID-19 of during the management period  $D(T)$ , the total number of people isolated at home or in hotels  $C_1$ , those who are hospitalized  $C_2$ , those who undertake the reverse transcription-polymerase chain reaction (RT-PCR) or antigen tests  $C_D$ , and the socio-economic cost caused by the behavioral restrictions  $C_f$ .

$C_1$  is calculated as the sum of isolated persons without any symptoms during the management period. Symptomatically infected persons are hospitalized if  $H_c(t) \geq H_2(t)$ . However, if the capacity of healthcare facilities is overwhelmed ( $H_c(t) < H_2(t)$ ), we assume that  $H_2(t) - H_c(t)$  persons are also isolated at home or in hotels. Then they are added to  $C_1$ .

$$C_1 = \int_0^T (H_{1a}(t) + H_{1b}(t) + \max\{H_2(t) - H_c(t), 0\}) dt \quad (8)$$

$C_2$  is the sum of hospitalized persons during the management period and is calculated as follows:

$$C_2 = \int_0^T \min\{H_2(t), H_c(t)\} dt \quad (9)$$

$C_D$  is the sum of the number of people who take the tests during the management period and is calculated as follows:

$$C_D = \frac{\theta}{\pi} \int_0^T (E(t) + I_{1a}(t) + I_{1b}(t)) dt \quad (10)$$

In reality, the rate of positive results fluctuates daily and may increase with the identification of infection clusters.



**Table 2** The list of parameters (The blank in the Reference column means that the value is an assumption.)

Symbol	Definition	Value	Reference
$N$	Total population in Tokyo on October 1, 2019	13 942 856	[55]
$\beta_1$	Asymptomatic infection rate		(derived from Eq. 4)
$\beta_2$	Symptomatic infection rate		(derived from Eq. 4)
$\gamma_1$	Recovery rate of asymptotically infected persons	$\gamma_1 \approx \gamma_{h1}$	
$1/\gamma_2$	Mean time from symptom onset to recovery	13.4	[5]
$1/\gamma_{h1}$	Average isolated period	10	[35]
$\gamma_{h2}$	Discharge rate from hospital	0.07	[36]
$1-p$	Proportion of asymptotically infected persons in all the infected persons	[0.1 : 0.5]	[4, 21, 42, 45]
$1/\eta$	Median of latent period	2.56	[51]
$1/\kappa$	Difference between the incubation period and the latent period	2.54	[31, 51]
$1/\lambda$	the time from the onset to hospitalization	2	
$\theta$	Detection rate of those who are exposed or asymptotically infected	[0 : 0.03]	
$\mathfrak{R}_0$	Basic reproduction number	2.6	[28, 56]
$H_c(t)$	Number of beds for infected persons to receive sufficient health care treatment at time $t$ in Tokyo	[3300 : 5594]	[37]
$\delta$	Case fatality rate	0.011 ...	[36]
$\pi$	Positive rate per RT-PCR test	0.05	[59]
$f_1$	$f$ during the emergency regulations of April-May in 2020 in Tokyo	0.6	[38]
$f_{max}$	$f$ the maximum degree of behavioral restrictions	0.6	
$T$	Management period from January 1, 2020 to May 14, 2021	500 days	
$T_1$	Response time	7 days	
$T_2$	The shortest execution time	14 days	
$\alpha$	Nonlinear effect for $C_f$	1	

For simplicity, it is assumed that  $\pi = 0.05$  is based on the data obtained from [59].

$C_f$  indicates the intensity of implemented behavioral restrictions and is calculated as follows:

**Table 3** The number of beds for infected persons to receive sufficient health care treatment in Tokyo,  $H_c(t)$  [37]

Day	Date (yyyy/mm/dd)	The number of beds
1 ~ 121	2020/01/01 ~ 2020/04/30	no data (assumed to be 3300)
122 ~ 245	2020/05/01 ~ 2020/09/01	3300
246 ~ 399	2020/09/02 ~ 2021/02/02	4000
400 ~ 413	2021/02/03 ~ 2021/02/16	4900
414 ~ 434	2021/02/17 ~ 2020/03/09	5000
435 ~ 483	2021/03/10 ~ 2021/04/27	5048
484 ~ 500	2021/04/28 ~ 2021/05/14	5594

$$C_f = \frac{1}{T} \int_0^T \left( \frac{f(t)}{f_{max}} \right)^\alpha dt \quad (11)$$

This indicator is an abstract non-dimensional measure and satisfies  $0 \leq C_f \leq 1$ .  $C_f = 0$  means that the usual state is maintained and  $C_f = 1$  does that the state of emergency is executed during the management period  $T$ .  $\alpha$  is the nonlinear effect. We assume that  $\alpha = 1$  in the manuscript and discuss cases of  $\alpha \neq 1$  in the [Supplementary file](#).

As two supplementary indicators,  $c_{r,max}$  and  $c_N$  are introduced to indicate the status of healthcare capacities.  $c_{r,max}$  is the maximum ratio of the number of occupied beds to the number of available beds for healthcare treatment during the management period, and is defined as follows:

**Table 4** Combinations of  $G_{up}$  and  $G_{down}$  for three scenarios: [A] To minimize the number of deaths  $D(T)$ , [B] To minimize the socio-economic cost  $C_f$ , [C] To minimize  $C_f$  under  $D(T) < 500$  and  $c_N = 0$

Scenario	[A]		[B]		[C]	
	$G_{up}$	$G_{down}$	$G_{up}$	$G_{down}$	$G_{up}$	$G_{down}$
1	0.05	0.05	0.95	0.60	0.45	0.25
2	0.05	0.05	1.00	0.95	0.35	0.70
3	0.05	0.05	1.00	0.60	0.65	0.35
4	0.05	0.05	1.00	0.65	0.95	0.15

$$c_{r,max} = \max c_r(t) = \max \left( \frac{H_2(t)}{H_c(t)} \right) \tag{12}$$

If  $c_{r,max} < G_{up}$ , then the state of emergency is not declared and there are no behavioral restrictions within the management period. Moreover, if  $c_{r,max} > 1$ , then the capacity of the healthcare facilities is overwhelmed at least once during this period.  $c_N$  is defined as the number of days in which  $c_r(t) > 1$  is true. Table 1 shows the list of variables, indicators and parameters.

### 2.4 Management parameter

We conduct the simulation, assuming our policy is implemented in Tokyo, Japan. Let  $N = 13\,942\,856$ , which supposes the population in Tokyo, Japan, on October 1, 2019, [55]. Parameters in Eq. 5 are determined as follows. Let  $1/\gamma_2 = 13.4$  days [5] and  $1/\gamma_{h1} = 10$  days [35].  $\gamma_{h2}$  is calculated as the ratio of those discharged from the hospital to inpatients, including death, in one day based on the data by [36], and our simulation employs  $\gamma_{h2} = 0.07$ . We assume that  $\gamma_1 \approx \gamma_{h1} = 0.1$  and  $\gamma_{h3} \approx \gamma_{h2} = 0.07$ . Let  $\lambda^{-1} = 2$ , and the sensitivity of  $D(T)$  and  $c_N$  to  $\lambda^{-1}$  is discussed in the Supplementary file. The asymptomatic ratio  $1 - p$  has been estimated by proposing various methods and using different data (e.g., [4, 21, 42, 45]). The estimated values range from 0.1 to 0.5; therefore, we assume that  $p$  ranges from 0.5 to 0.9 and let  $p = 0.7$ . The latent period

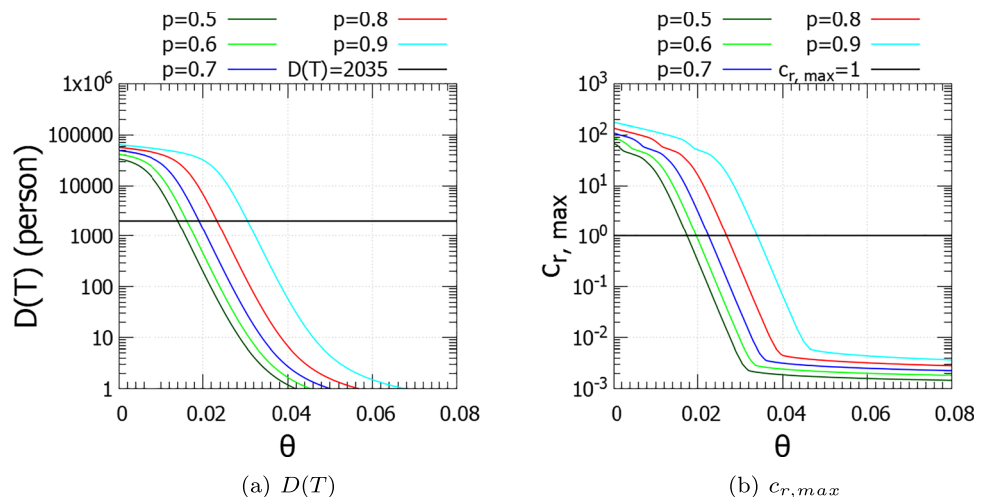
$\eta^{-1} = 2.56$  days [51], and the incubation period was 5.1 days [31]. Thus, let  $\kappa^{-1} = 5.1 - 2.56 = 2.54$  days. We assume that the management period is 500 days ( $T = 500$ ) from January 1, 2020, to May 14, 2021, as the vaccination for people over 64 years of age was issued in Japan on April 12, 2021, and the vaccine doses per capita have rapidly increased since the middle of May [46].

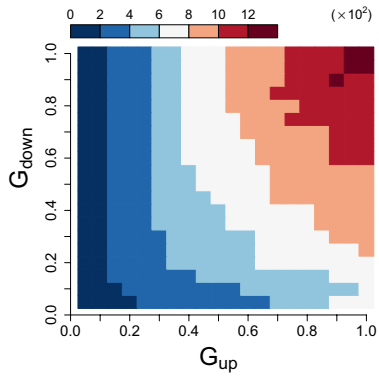
In reality, the fatality rate depends on symptoms, age, and access to appropriate medical care [64]. However, it is assumed to be a constant in this paper. According to the data [36], the number of confirmed cases is 77853 from June 1, 2020, to May 31, 2021, while that of fatalities in the same period is 875. Thus, we obtain  $\delta = 875/77853 = 0.011 \dots$

Some studies report that the estimated value of the basic reproduction number, defined as the average number of secondary cases generated by a typical primary case in an entirely susceptible population, varies widely from country to country [32, 53]. The basic reproduction number for the epidemic in Japan was also estimated (e.g., [28, 56]). Kuniya [28] reported that it was  $\mathfrak{R}_0 = 2.6$  whose 95% confidence interval was 2.4 to 2.8, and therefore, we adopt  $\mathfrak{R}_0 = 2.6$  in this paper. Table 2 shows the list of parameters.

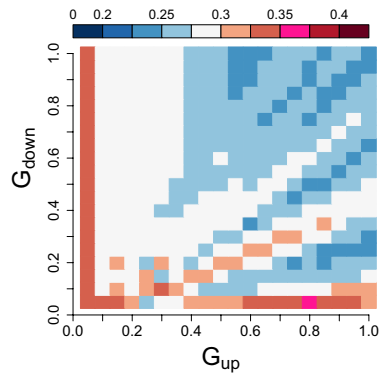
Table 3 shows the number of beds available for healthcare treatment in Tokyo, Japan. The number of beds available for healthcare treatment has increased [37]. Although data on the number of beds is missing from January 1, 2021, to April 30, 2021, we assume  $H_c(t) = 3300$  during this period.

**Fig. 2** (a) The number of cumulative deaths by COVID-19  $D(T)$  and (b)  $c_{r,max}$  with different  $\theta$  when  $f = 0$  and  $\lambda^{-1} = 2$  at any time  $t$

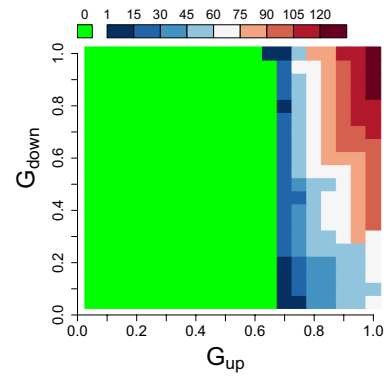




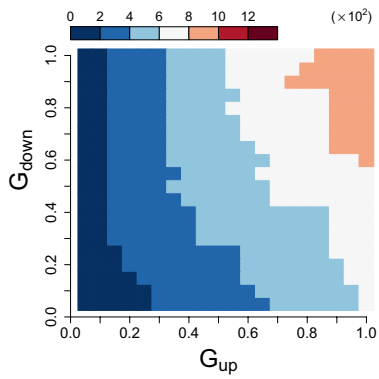
(a)  $D(T)$  (1-level)



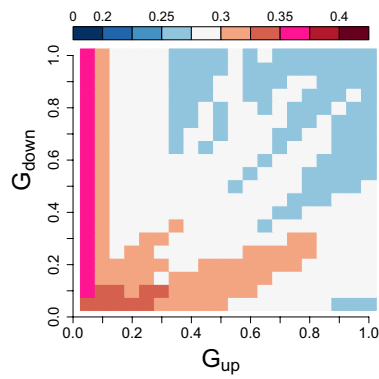
(b)  $C_f$  (1-level)



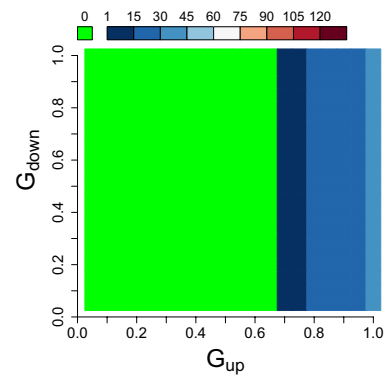
(c)  $c_N$  (1-level)



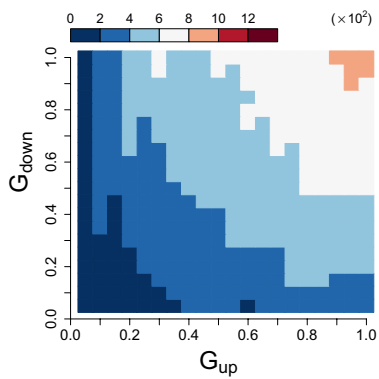
(d)  $D(T)$  (2-level)



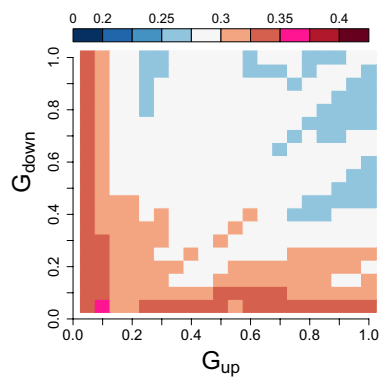
(e)  $C_f$  (2-level)



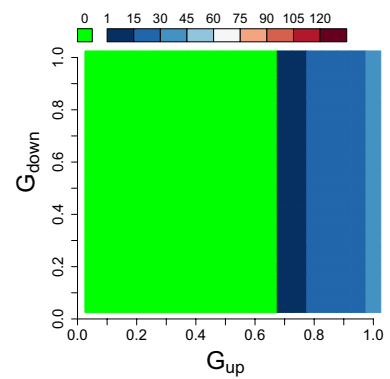
(f)  $c_N$  (2-level)



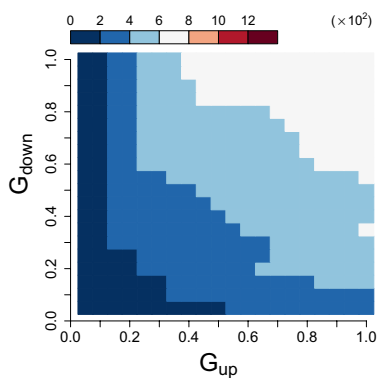
(g)  $D(T)$  (3-level)



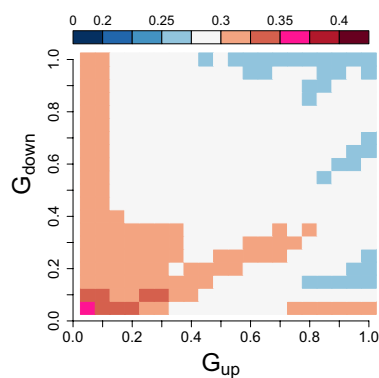
(h)  $C_f$  (3-level)



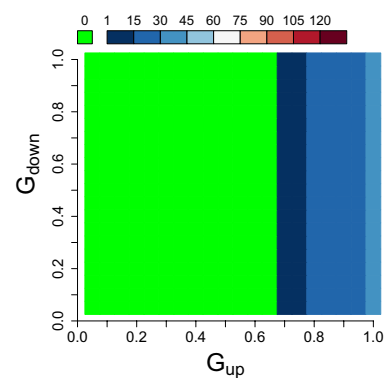
(i)  $c_N$  (3-level)



(j)  $D(T)$  (4-level)



(k)  $C_f$  (4-level)



(l)  $c_N$  (4-level)



**Fig. 3** Heat maps of the cumulative number of deaths by COVID-19  $D(T)$ , the socio-economic cost caused by the behavioral restrictions  $C_f$ , and the number of days in which the capacity of health care facilities is overwhelmed  $c_N$  when  $p = 0.7$  and  $\theta = 0$ . Their units are person, no dimension, and day, respectively

## 2.5 Simulation

First, we investigated the behavior of the SEIIHHHR model without feedback control over the degree of behavioral restrictions. The simulations were conducted under  $f(t) = 0$ , and the sensitivities of  $D(T)$  and  $c_{r,max}$  were analyzed in relation to  $\theta$ . Second, we conducted simulations with different combinations of  $G_{up}$  and  $G_{down}$  and verified whether feedback control can be effective in reducing  $D(T)$ ,  $C_f$ , and  $c_N$ . Third, based on the combinations of  $G_{up}$  and  $G_{down}$ , we considered three different scenarios: [A] to minimize  $D(T)$ , [B] to minimize  $C_f$ , and [C] to minimize  $C_f$  under  $D(T) < 500$  and  $c_N = 0$ . Table 4 shows combinations of  $G_{up}$  and  $G_{down}$  which achieved the goal of the three scenarios when  $\theta = 0$  and  $p = 0.7$ . The strategic planning for achieving scenario A is to initiate behavioral restrictions early and maintain them until the occupied ratio of beds available for healthcare treatment is reduced. In contrast, behavioral restrictions in scenario B are reinforced when the number of hospitalized people increases while scenario C is an intermediate strategy. Using these arrangements, we investigated the level of feedback control that is more effective in reducing the indicators referred to in the previous subsection with different values of  $\theta$ . Finally, we explored the performance of feedback control when  $\theta$  is governed by a uniform distribution with different  $p$  values ranging from 0.5 to 0.9.  $\theta = \theta(t)$  varies on a daily basis and ranges from [0.0, 0.03]. Trials were carried out 1000 times and the statistical values were obtained.

The simulation starts from  $S(0) = N - 10$ ,  $E(0) = 10$ , and  $I_1(0) = I_2(0) = H_1(0) = H_2(0) = H_3(0) = R(0) = 0$ . The first deceased person due to COVID-19 was confirmed on February 26, 2020, [60]. In Tokyo, 2035 people died of the infection, and the total period of the state of emergency was 147 days by May 14, 2021, [36].

## 3 Results

Figure 2 shows  $D(T)$  and  $c_{r,max}$  with different detection rate  $\theta$  for  $f = 0$  during the management period. Both  $D(T)$  and  $c_{r,max}$  are monotonically decreasing with  $\theta$ , and they are larger as the symptomatic rate  $p$  becomes higher. For  $p = 0.7$  as shown in Fig. 2(a), if  $\theta \geq 0.0195$  throughout the management period,  $D(T)$  will be lower than the actual data even without any behavioral restrictions. Moreover, according to Fig. 2(b), the capacity of health care capacity will be overwhelmed if  $\theta \leq 0.034$  for  $p = 0.9$ . This figure suggests that

the detection of infected persons should be strengthened to contain the epidemic when  $p$  is high.

Figure 3 demonstrates the results of simulations with  $p = 0.7$  and different combinations of  $G_{up}$  and  $G_{down}$  using three different indicators:  $D(T)$ ,  $C_f$ , and  $c_N$ . Since these simulations were conducted under  $\theta = 0$ , the total number of those who take the test to detect infected persons,  $C_D$ , is zero for any combinations. Decreasing  $G_{up}$  and  $G_{down}$  contribute to reducing  $D(T)$ , as shown in Fig. 3(a), (d), (g), and (j). When  $G_{up}$  and  $G_{down}$  are high,  $D(T)$  rises especially, in the 1-level.

When it comes to  $C_f$  shown in Figure 3(b), (e), (h), and (k), the same colored clusters radiate from the origin. The figures show a combination of high  $G_{up}$  and  $G_{down}$  is effective in reducing  $C_f$ , especially in the lower level feedback control. When  $G_{up} = 0.05$ ,  $C_f$  is large in all the levels of the feedback control.

As shown in Fig. 3(c), (f), (i), and (l), a low  $G_{up}$  reduces the risk that the capacity of health care facilities is overwhelmed. In the case of  $p = 0.7$ ,  $G_{up} < 0.7$  is favorable for keeping the health care system with the exception of some combinations of the 1-level. In addition, the  $c_N$  of the 1-level trends to be much longer than those in the other levels when  $G_{up} \geq 0.7$ .

Combinations of  $G_{up}$  and  $G_{down}$  are selected so that the indicators can be reduced. Table 4 shows the best combinations of  $G_{up}$  and  $G_{down}$  for each scenario when  $\theta = 0$ . Figures 4, 5, and 6 demonstrate the sensitivity analysis in relation to  $\theta$  for three different scenarios. The combinations of  $G_{up}$  and  $G_{down}$  are fixed regardless of the value of  $\theta$  in the simulation. In each figure, panel (a), (b), (c), (d), (e), and (f) show  $D(T)$ ,  $C_f$ ,  $C_1$ ,  $C_2$ ,  $C_D$ , and  $c_N$ , respectively.

For scenario A shown in Fig. 4, the  $D(T)$  is under 100 persons in all the levels. The  $C_f$  of the 1-level is lower than those of multilevel controls. In  $\theta \geq 0.0295$ , behavioral restrictions are not implemented and  $D(T)$  corresponds to the line of  $p = 0.7$  of Fig. 2. The  $C_1$  and  $C_D$  are increasing as  $\theta$  is raised. The behaviors of  $C_1$  and  $C_D$  are similar and  $C_D$  is about three times larger than  $C_1$ . In addition, the behavior of the total number of hospitalized persons,  $C_2$ , is also similar to that of  $D(T)$ . As  $\theta$  becomes larger, the period of behavioral restrictions is shorter and its initiation is delayed. Thus, the  $D(T)$  and  $C_2$  rise in  $0.02 \leq \theta \leq 0.0295$ .  $c_N = 0$  is maintained regardless of  $\theta$  in all the levels and the capacity of health care facilities is enough for scenario A.

For scenario B shown in Fig. 5, the  $C_f$  is under 0.27 in all the levels, and however, the other indicators are about 10 times larger than those of scenario A. In the 1-level, the  $C_f$  is the lowest and the other indicators are the largest of all the levels. The  $c_N$  of the 4-level is the same as those of the 2- and 3-level and overlaps with them in Fig. 5(f). When  $\theta = 0$ ,  $c_N$  is 83 days in the 1-level and is 31 days in the other levels. This implies that many symptomatically infected persons cannot be hospitalized and are isolated at home or in hotels. The  $c_N$  is roughly decreasing with increasing  $\theta$ , and however,  $\theta \geq 0.0225$  should be maintained to achieve  $c_N = 0$  during

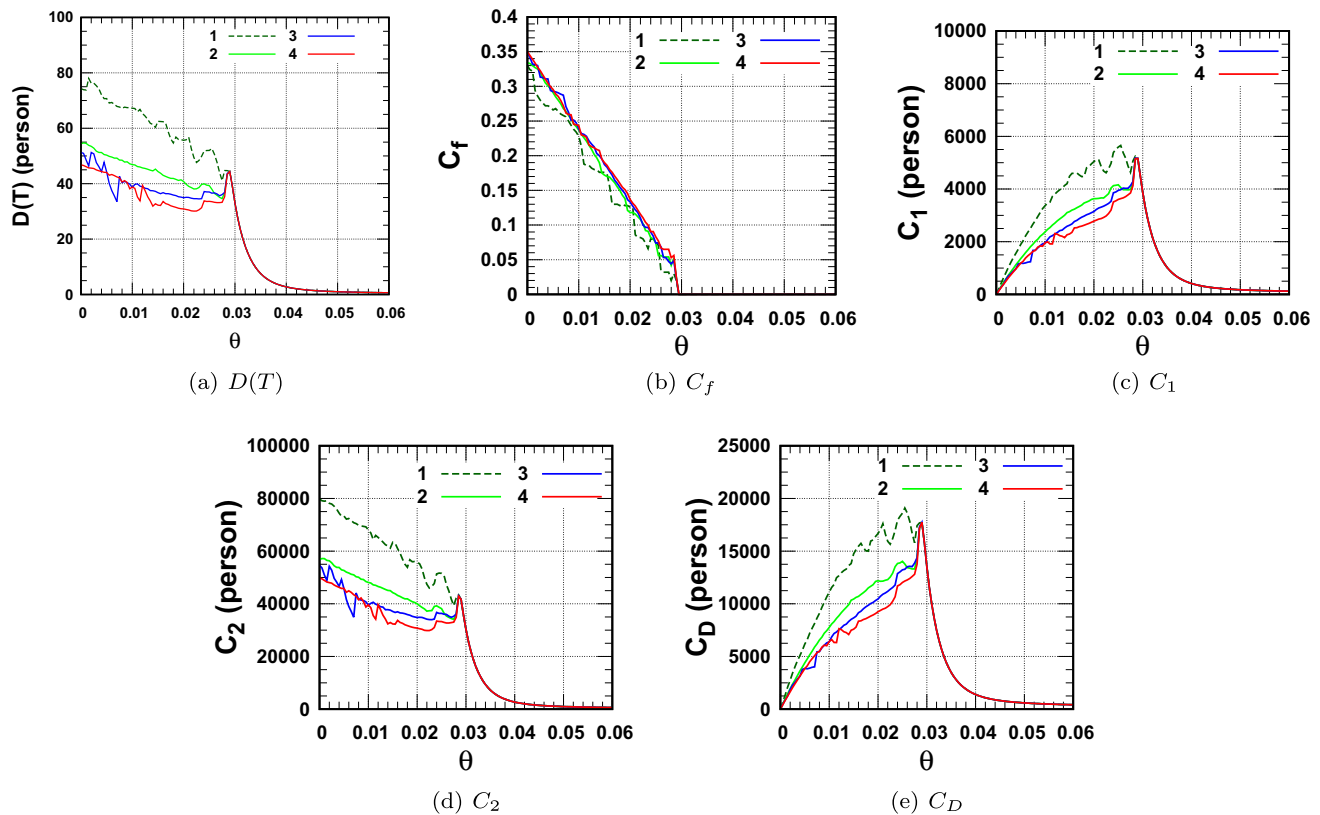


**Fig. 4** Sensitivity of indicators for scenario A in relation to  $\theta$  when  $p = 0.7$ .  $c_N = 0$ , regardless of  $\theta$ , in all feedback controls

the management period. The  $D(T)$  and  $C_2$  of the 3-level surge and drop sharply in  $0.003 \leq \theta \leq 0.007$ .

Figure 6 shows the result of scenario C.  $D(T)$ ,  $C_1$ ,  $C_2$ , and  $C_D$  of the 4-level are the smallest in  $0 \leq \theta < 0.02$ , while those of the 2-level are the smallest in  $\theta \geq 0.02$ . The  $D(T)$  of the 2-level exceeded 500 persons in  $0.001 \leq \theta \leq 0.006$ . The  $C_f$  of the 4-level slightly decreases in  $0.012 \leq \theta \leq 0.021$  and keeps high, compared with the other levels. At  $\theta = 0.02$ , although the difference of  $D(T)$  of the 4- and 2-levels is just 3 (= 253 – 250) persons, their  $C_f$  are 0.137 and 0.068, respectively.

Figure 7 shows the sensitivity analysis in relation to  $p$  for three different scenarios when  $\theta$  fluctuates on a daily basis.  $D(T)$ ,  $C_f$ , and  $C_D$  are shown in the figure, and  $C_1$ ,  $C_2$ , and  $c_N$  are discussed in the [Supplementary file](#). For scenario A shown in Fig. 7(a), (b), and (c), means of  $D(T)$  are almost constant and differences between the maximum and the minimum of  $D(T)$  are small in all the level. Means of  $C_f$  are increasing and those of  $C_D$  are decreasing with increasing  $p$ . The mean of  $C_f$  in the 1-level is the smallest and the  $D(T)$  is the largest. In contrast, the 4-level resulted in the largest  $C_f$  and the smallest  $D(T)$ .

For scenario B shown in Fig. 7(d), (e), and (f), means of  $D(T)$  in the 1- and 2-levels are increasing as  $p$  becomes larger unlike scenario A. On the other hand, means of  $C_f$  are increasing as  $p$  becomes larger, like scenario A. Means of  $C_D$  are also decreasing with increasing  $p$  for multilevel feedback controls. However, the mean of  $C_D$  in the 1-level rises at  $p = 0.7$ .

Panels (g), (h), and (i) in Fig. 7 show the result of scenario C. Means of  $D(T)$  and  $C_D$  for the 4-level are the smallest with the exception of  $p = 0.5$ . The  $C_f$  is higher in the 4-level, and however, differences of the means between the 4-level and the other levels are decreasing with increasing  $p$ . According to  $D(T)$ ,  $C_f$ , and  $C_D$ , the 4-level is relatively effective when  $p$  is high.

## 4 Discussion

We established the SEIIHHHR model as a mathematical epidemic model of the COVID-19 and calculated indicators such as the socio-economic cost caused by the behavioral restrictions  $C_f$ , the total number of those who are isolated at home or in hotels  $C_1$ , the total number of hospitalized persons  $C_2$ , and the total number of those who take the test to detect infected persons  $C_D$  as well as the cumulative number of infected deaths  $D(T)$ . We conducted numerical simulations of implementing nonpharmaceutical interventions such as detecting infected persons in public spaces and restricting people's activities. The RT-PCR testing is not only a monitoring but also an intervention measure. As a result of simulations with different detection rate  $\theta$ ,  $D(T)$  and the burden on the health care system are reduced as  $\theta$  becomes larger. To develop a measure against the virus with uncertain symptomatic rate, we proposed a feedback control

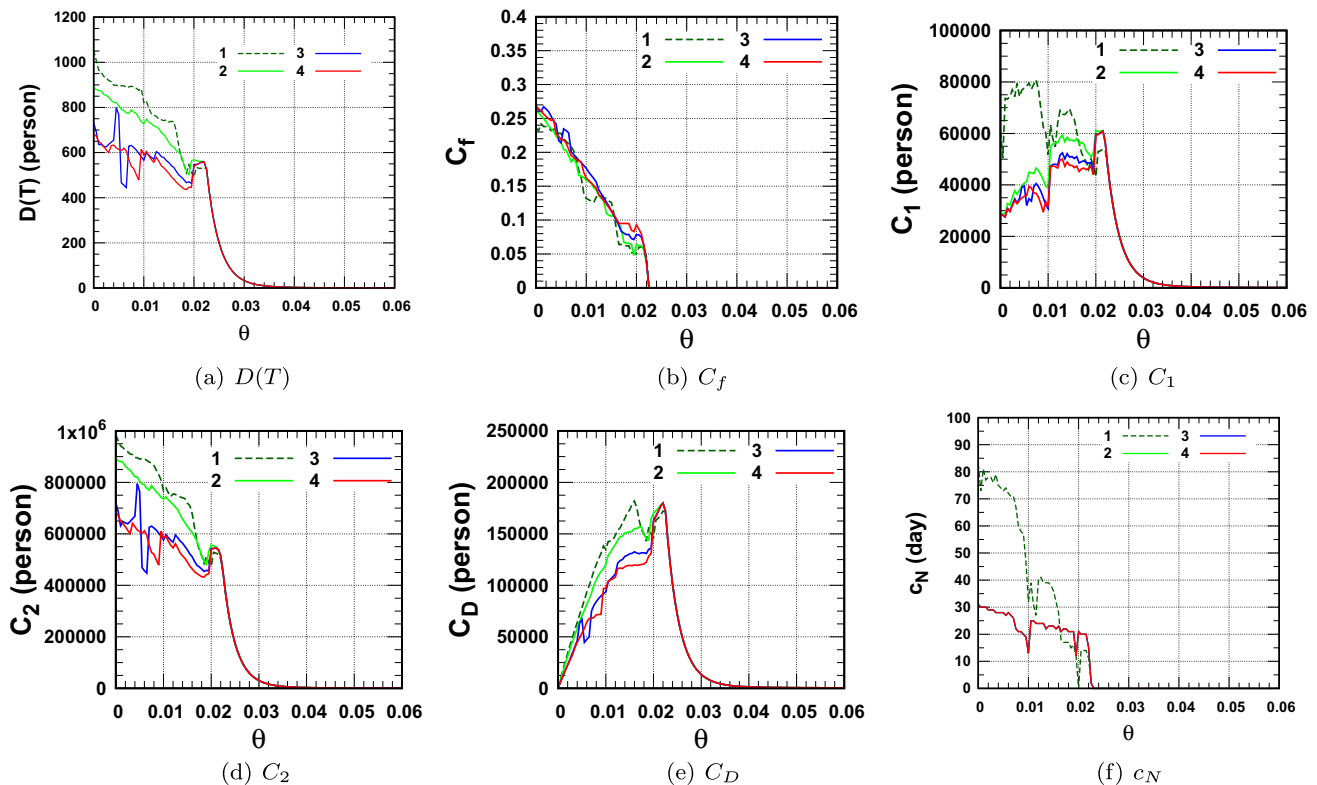


**Fig. 5** Sensitivity of indicators for scenario B in relation to  $\theta$  when  $p = 0.7$ . The result of  $c_N$  in the 4-level overlaps with those in the 2- and 3-level

of the degree of behavioral restrictions  $f$ . The  $f$  in the feedback control is adapted for how many infected persons occupy the health care facility and its trend. We concluded the feedback control of  $f$ , rather than fixing  $f$ , can reduce  $D(T)$  and other costs to take countermeasures against the virus.

One of the simplest feedback controls is the bang-bang control (1-level) which repeats the state of emergency and the usual state. We explored a better way and suggested the multilevel feedback control in which the band of changing  $f$  is narrowed. Three different scenarios were prepared for our simulations by exploring combinations of two parameters  $G_{up}$  and  $G_{down}$ . We came to some conclusions from the simulations. We found out that increasing  $G_{up}$  and  $G_{down}$  reduces  $C_f$ , whereas decreasing  $G_{up}$  and  $G_{down}$  does  $D(T)$ . The number of days in which the capacity of health care facilities is overwhelmed  $c_N$  depends on  $G_{up}$  regardless of the number of levels for feedback control. The result of scenario A implied that early initiating and maintaining behavioral restrictions can be reasonable to decrease indicators except for  $C_f$ . Furthermore, the  $D(T)$  in scenario A does not rise so much if the proportion of infected persons who develop symptoms  $p$  is high. Gevertz et al. [19] investigated the best timing of initiating and canceling physical distancing and argued that it should start early and relax slowly. Our finding follows this research. According to Figs. 4 and 5, scenario A reduced  $D(T)$ ,  $C_1$ ,  $C_2$ , and  $C_D$  to about one tenth of those of

scenario B. On the other hand, its  $C_f$  is larger by 0.08 than that of scenario B. From these two scenarios, the bang-bang control seemed to be better to reduce  $C_f$ . However, it must be noted that  $C_f$  is an abstract measure and the cost to raise  $f$  is assumed to be linear. The cost to increase  $f$  includes the monetary compensation for businesses damaged by the governmental interventions. A multilevel feedback control is preferable to reduce  $D(T)$ ,  $C_1$ ,  $C_2$ , and  $C_D$ . In scenario C, the 4-level feedback control is effective when  $p$  is high. As  $p$  becomes higher,  $C_f$  is increasing and  $C_D$  is decreasing. The  $C_1$ ,  $C_2$ , and  $C_D$  can be converted into money by multiplying each cost per person. Depending on their unit costs, the favorable scenario may be changed.

Our analysis has several limitations. This paper assumed the distribution of population is homogeneous while that in reality is heterogeneous. We did not consider other important factors such as the time delay for aggravation of symptoms, the age group of patients, the increase of the number of suicides caused by recession, and the influence of superspreading events reported in [44]. The Japanese government counts the number of deceased individuals who were positive for COVID-19 reported by jurisdictions, and defines it as infected deaths by COVID-19 without specifying the cause of death. However, we calculated the number of infected deaths in those who are newly confirmed cases in the management period. We do not consider how or to what extent we can increase  $\theta$ . The

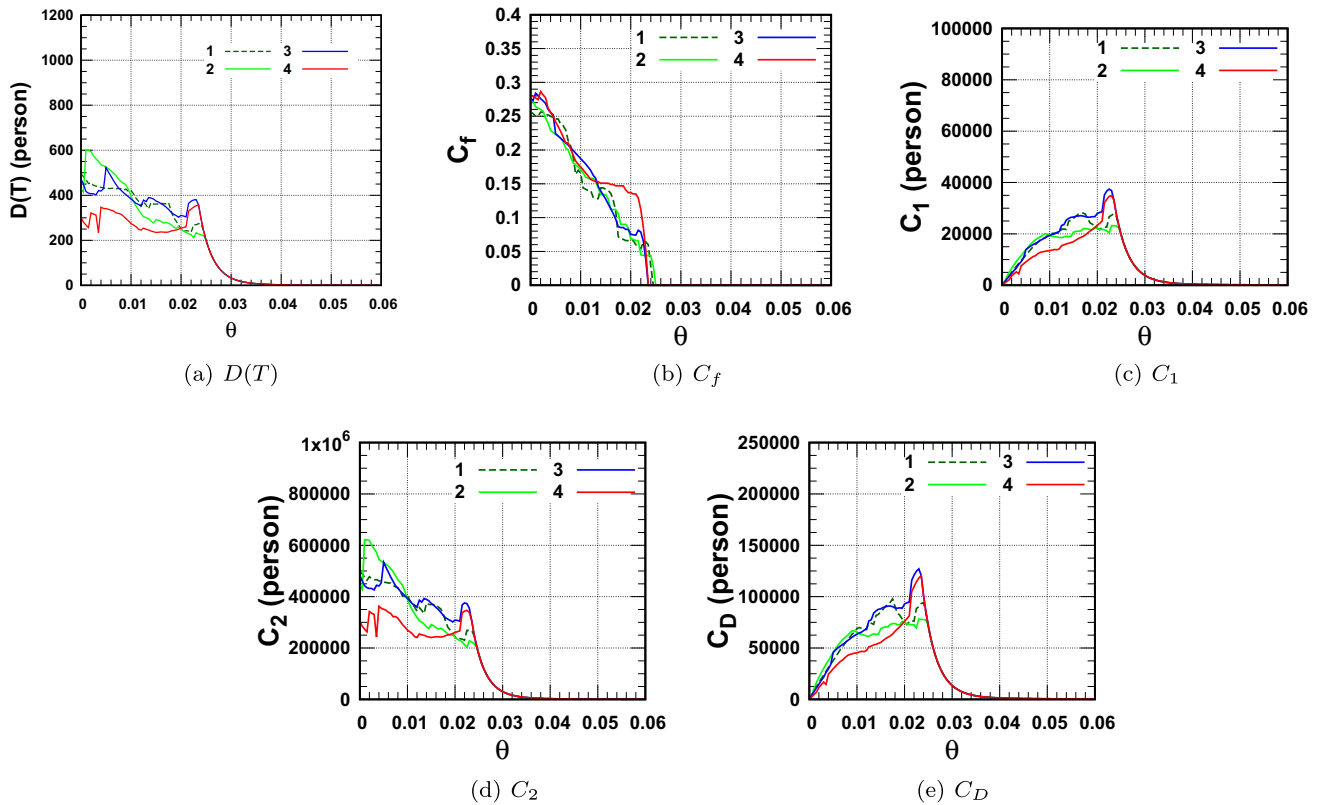


**Fig. 6** Sensitivity of indicators for scenario C in relation to  $\theta$  when  $p = 0.7$ ,  $c_N = 0$ , regardless of  $\theta$ , in all feedback controls

number of beds in health care facilities for infected persons with symptoms  $H_c(t)$  is assumed to be the same as the actual data during the management period in our simulation, but its increase may be also effective in reducing indicators [10, 65].

The timing of reinforcing or relaxing the behavioral restrictions might be more effective by using other indicators, such as the reduction in individual consumption due to the restrictions, the estimated number of unconfirmed infections, the number of severely ill persons, the number of deaths, or the positive rate of the test. Their combinations can be effective because indicators were sometimes unstable as shown in in Figs. 4, 5, and 6. In addition, we assumed a time lag of one week because immediate executing or canceling behavioral restrictions may be impossible. If we could reduce the time lag of policy change, we would manage the situation more effectively.

We ignored a possibility that a successive long strong behavioral restriction causes the bankruptcy of business for which remote work cannot be substituted. The COVID-19 cases resurged in Japan from November, 2020 to January, 2021, [1, 27], and the number of infected deaths also increased in Tokyo [60]. Karako et al. [27] argued that this was because people seemed accustomed to the situation of this epidemic and their level of activity was not reduced during the period. In Japan, no legal penalties are imposed for violating behavioral restrictions called for by the government. In this study, we didn't consider such people's

spontaneous behavior change and assumed the degree of behavioral restrictions changes discretely and keeps constant during a certain period in the feedback control. However, people may reduce their mobility restrictions by themselves even though some governmental interventions are being implemented [41, 49]. From a point of view of behavioral science, Atkinson-Clement and Pigalle [2] argued that a lack of trust towards government measures reduces compliance. The management period of the simulation is from January 1, 2020 to May 14, 2021, but the outbreak of the SARS-CoV-2 Alpha variants, which has a higher transmissibility [57], was not considered.

The framework in the present study can be applied to another infectious disease against which vaccines and specific medicines are not developed in the future. A feedback controller approach is an effective way even after vaccines and specific medicines are developed because of the resurgence of infection cases caused by the loss of immunity. However, the knowledge provided by these models can only be understood in terms of the dynamical system. The structure of the model and its parameters need to be validated and improved in response to the appearance of variants which have different properties and the development of pharmaceutical interventions. Moreover, it must be stressed that if the value of statistical life is not converted to economic loss, then there is no objective optimal solution and that evaluations made during the decision-making process are arbitrary. The Japanese government

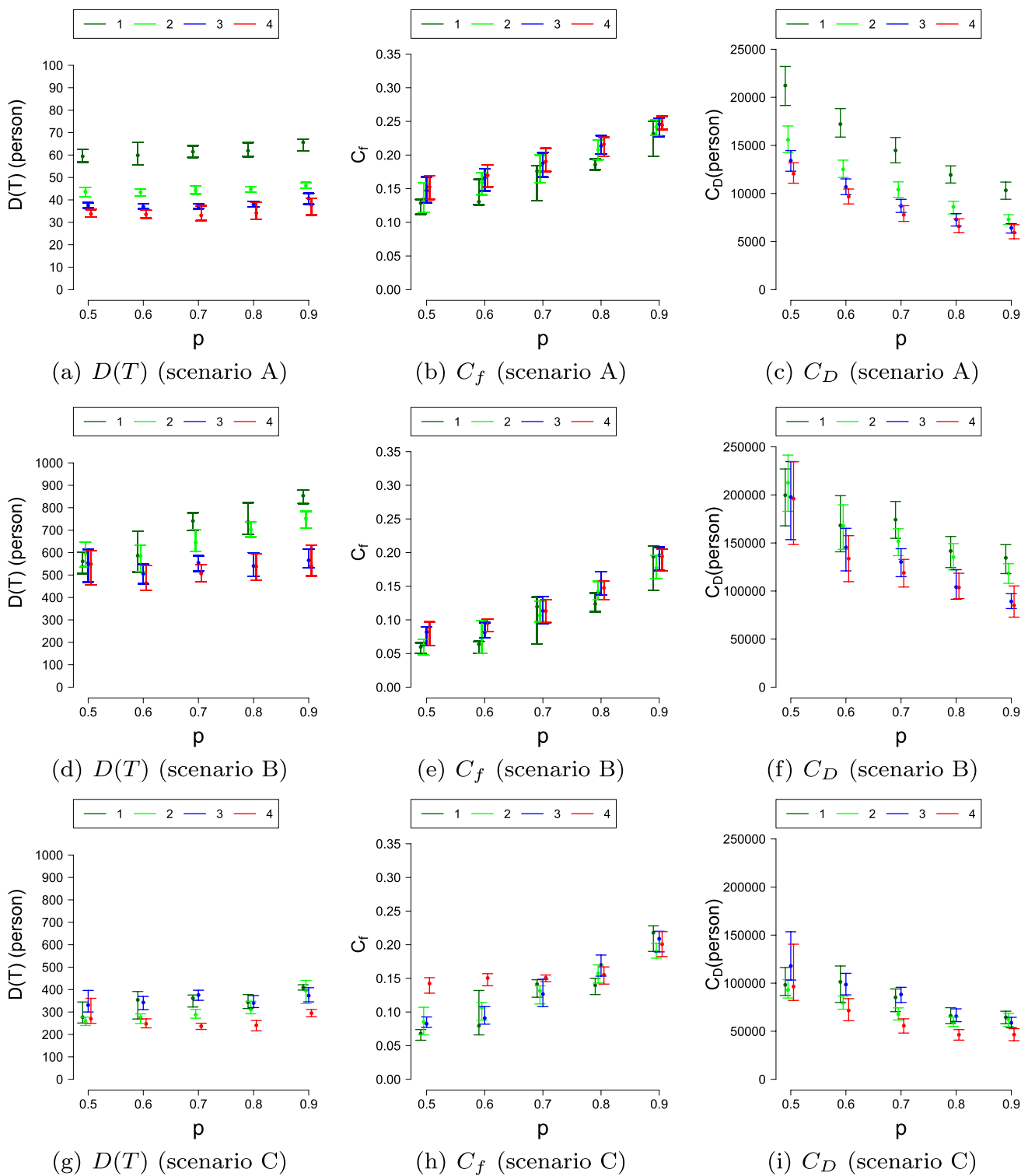


**Fig. 7** Sensitivity of indicators for scenario A (panels (a), (b), and (c)), B (panels (d), (e), and (f)), and C (panels (g), (h), and (i)) in relation to  $p$ . Point indicates the mean value. The upper and lower bars show the maximum and minimum values, respectively

was late to start administering the COVID-19 vaccination, but the vaccine doses per capita have been rapidly increasing since the middle of May, 2021 [46]. We will consider a better measure

against the epidemic under insufficient data and cost-effectiveness of a variety of anti-contagion measures including pharmaceutical interventions such as vaccination.

### Appendix A: Derivation of basic reproduction number $\mathfrak{R}_0$

The basic reproduction number is derived from Eq. 1 as follows:

$$\begin{cases} \frac{dS}{dt} = -(\beta_1(I_{1a} + I_{1b}) + \beta_2 I_2) \frac{S}{N} \\ \frac{dE}{dt} = (\beta_1(I_{1a} + I_{1b}) + \beta_2 I_2) \frac{S}{N} - \eta E \\ \frac{dI_{1a}}{dt} = \eta(1 - p)E - \gamma_1 I_{1a} \\ \frac{dI_{1b}}{dt} = \eta p E - \kappa I_{1b} \\ \frac{dI_2}{dt} = \kappa I_{1b} - \gamma_2 I_2 \\ \frac{dR}{dt} = \gamma_1 I_{1a} + \gamma_2 I_2 \end{cases} \quad (A1)$$

The linearized system at the disease-free steady state for Eq. 1 is

$$\frac{d}{dt} \begin{bmatrix} u \\ v \\ w \\ x \end{bmatrix} = (M + Q) \begin{bmatrix} u \\ v \\ w \\ x \end{bmatrix} \quad (A2)$$

where  $u, v, w,$  and  $x$  denote the linearized forms of  $E, I_{1a}, I_{1b},$  and  $I_2,$  respectively. And

$$M = \begin{bmatrix} 0 & \beta_1 & \beta_1 & \beta_2 \\ 0 & 0 & 0 & 0 \\ 0 & 0 & 0 & 0 \\ 0 & 0 & 0 & 0 \end{bmatrix}, Q = \begin{bmatrix} -\eta & 0 & 0 & 0 \\ \eta(1-p) & -\gamma_1 & 0 & 0 \\ \eta p & 0 & -\kappa & 0 \\ 0 & 0 & \kappa & -\gamma_2 \end{bmatrix} \quad (A3)$$

The next generation matrix with large domain  $K$  is calculated as

$$K = -MQ^{-1} = \begin{bmatrix} (1-p)\frac{\beta_1}{\gamma_1} + p\frac{\beta_1}{\kappa} + p\frac{\beta_2}{\gamma_2} & \frac{\beta_1}{\gamma_1} & \frac{\beta_1}{\gamma_1} + \frac{\beta_2}{\gamma_2} & \frac{\beta_2}{\gamma_2} \\ 0 & 0 & 0 & 0 \\ 0 & 0 & 0 & 0 \\ 0 & 0 & 0 & 0 \end{bmatrix} \quad (A4)$$

The basic reproduction number  $\mathfrak{R}_0$  is equivalent to the spectral radius of  $K.$

$$\mathfrak{R}_0 = (1-p)\frac{\beta_1}{\gamma_1} + p\frac{\beta_1}{\kappa} + p\frac{\beta_2}{\gamma_2} \quad (A5)$$

### Appendix B: Algorithm for the feedback control

```

1:  $H_{2,j}$ , and  $H_{c,j}$  denotes  $H_2$  and  $H_c$  at the  $j$ th day.  $c_{r,j} = H_{2,j}/H_{c,j}$ .  $H_{2,0} = 0, H_{c,0} = 3300$  state = 0, counta = 0, countb = 0,  $f = 0, DF = f_{max}/Level$ , and  $f_{max} = f_1 = 0.6$ .  $\lfloor \cdot \rfloor$  denotes the floor function.
2: for  $j = 1$  to  $T$  do
3:   if state = 0 then
4:     if  $c_{r,j} > G_{up}$  and  $\dot{H}_{2,j} > 0$  then
5:       state = 1, counta = 0
6:     end if
7:   else if state = 1 and counta =  $T_1$  then
8:      $f = f_{max}, \Delta f = \lfloor 0.5 \times Level \rfloor \times DF$ , state = 2, countb = 0
9:   else if state = 2 and countb  $\geq T_2$  then
10:    if  $f + \Delta f \leq f_{max}, c_{r,j} > \left(\frac{f + \Delta f}{f_{max}}\right) \times G_{up}$ , and  $\dot{H}_{2,j} > 0$  then
11:      state = 3, counta = 0
12:    else if  $f - \Delta f \geq 0, c_{r,j} \leq \left(\frac{f}{f_{max}}\right) \times G_{down}$ , and  $\dot{H}_{2,j} < 0$  then
13:      state = 4, counta = 0
14:    end if
15:   else if state = 3 and counta =  $T_1$  then
16:      $f = f + \Delta f$ , state = 2, countb = 0,
17:     if  $\Delta f > DF$  then
18:        $\Delta f = \Delta f - DF$ 
19:     end if
20:   else if state = 4 and counta =  $T_1$  then
21:      $f = f - \Delta f$ , state = 2, countb = 0
22:     if  $\Delta f > DF$  then
23:        $\Delta f = \Delta f - DF$ 
24:     end if
25:   end if
26:   counta = counta + 1, countb = countb + 1
27: end for
28: return

```

**Supplementary Information** The online version contains supplementary material available at <https://doi.org/10.1007/s10729-022-09617-0>.

**Funding** No funding was received for conducting this study.

**Data availability** Not applicable

**Code availability** The simulation code was available in the Supplementary material.

#### Declarations

**Conflicts of interest** The authors have no conflicts of interest to declare that are relevant to the content of this article.



## References

- Arima Y, Kanou K, Arashiro T, Ko Y, Otani K, Tsuchihashi Y, Takahashi T, Miyahara R, Sunagawa T, Suzuki M (2021) Epidemiology of coronavirus disease 2019 in Japan: descriptive findings and lessons learned through surveillance during the first three waves. *JMA Journal* 4:198–206. <https://doi.org/10.31662/jmaj.2021-0043>
- Atkinson-Clement C, Pigalle E (2021) What can we learn from Covid-19 pandemic's impact on human behaviour? The case of France's lockdown. *Humanit Soc Sci Commun* 8. <https://doi.org/10.1057/s41599-021-00749-2>
- Basnarkov L (2021) Chaos, Solitons and Fractals 142. SEAIR Epidemic spreading model of COVID-19. 110394. <https://doi.org/10.1016/j.chaos.2020.110394>
- Byambasuren O, Cardona M, Bell K, Clark J, McLaws M, Glasziou P (2020) Estimating the extent of asymptomatic COVID-19 and its potential for community transmission: systematic review and meta-analysis. *Official Journal of the Association of Medical Microbiology and Infectious Disease Canada*. <https://doi.org/10.3138/jammi-2020-0030>
- Byrne AW, McEvoy D, Collins AB, Hunt K, Casey M, Barber A, Butler F, Griffin J, Lane EA, McAloon C, O'Brien K, Wall P, Walsh KA, More SJ (2020) Inferred duration of infectious period of SARS-CoV-2: rapid scoping review and analysis of available evidence for asymptomatic and symptomatic COVID-19 cases. *BMJ Open* 10. <https://doi.org/10.1136/bmjopen-2020-039856>
- Bohk-Ewald C, Dudel C, Myrskylä M (2020) A demographic scaling model for estimating the total number of COVID-19 infections. *Int J Epidemiol* 49:1963–1971. <https://doi.org/10.1093/ije/dyaa198>
- Böhning D, Rocchetti I, Maruotti A, Holling H (2020) Estimating the undetected infections in the Covid-19 outbreak by harnessing capture-recapture methods. *Int J Infect Dis* 97:197–201. <https://doi.org/10.1016/j.ijid.2020.06.009>
- Cabinet Secretariat, Government of Japan (2021). <https://corona.go.jp/en/emergency/>. Accessed 13 Sept 2022
- Choi W, Shim E (2021) Optimal strategies for social distancing and testing to control COVID-19. *J Theor Biol* 512:110568. <https://doi.org/10.1016/j.jtbi.2020.110568>
- Currie CSM, Fowler JW, Kotiadis K, Monks T, Onggo BS, Robertson DA, Tako AA (2020) How simulation modelling can help reduce the impact of COVID-19. *J Simul* 14:89–37. <https://doi.org/10.1080/17477778.2020.1751570>
- Davies NG, Kucharski AJ, Eggo RM, Gimma A, Edmunds WJ (2020) Effects of non-pharmaceutical interventions on COVID-19 cases, deaths, and demand for hospital services in the UK: a modelling study. *Lancet Public Health* 5:e375–e385. [https://doi.org/10.1016/S2468-2667\(20\)30133-X](https://doi.org/10.1016/S2468-2667(20)30133-X)
- Di Lauro F, Kiss IZ, Miller JC (2021) Optimal timing of one-shot interventions for epidemic control. *PLoS Comput Biol* 17:1–25. <https://doi.org/10.1371/journal.pcbi.1008763>
- Dias S, Queiroz K, Araujo A (2021) Controlling epidemic diseases based only on social distancing level. *Journal of Control, Automation and Electrical Systems*. <https://doi.org/10.1007/s40313-021-00745-6>
- Flaxman S, Mishra S, Gandy A, Unwin HJT, Mellan TA, Coupland H, Whittaker C, Zhu H, Berah T, Eaton JW, Monod M, Imperial College COVID-19 Response Team, Ghani AC, Donnelly CA, Riley S, Vollmer MAC, Ferguson NM, Okell LC, Bhatt S (2020) Estimating the effects of non-pharmaceutical interventions on COVID-19 in Europe. *Nature* 584:257–261. <https://doi.org/10.1038/s41586-020-2405-7>
- Ferguson NM, Cummings DAT, Cauchemez S, Fraser C, Riley S, Meeyai A, Iamsirithaworn S, Burke DS (2005) Strategies for containing an emerging influenza pandemic in southeast Asia. *Nature* 437:209–214. <https://doi.org/10.1038/nature04017>
- Ferguson NM, Cummings DAT, Fraser C, Cajka JC, Cooley PC, Burke DS (2006) Strategies for mitigating an influenza pandemic. *Nature* 442:448–452. <https://doi.org/10.1038/nature04795>
- Ferguson NM, Laydon D, Nedjati-Gilani G, Imai N, Ainslie K, Baguelin M, Bhatia S, Boonyasiri A, Cucunubá Z, Cuomo-Dannenburg G, Dighe A, Dorigatti I, Fu H, Gaythorpe K, Green W, Hamlet A, Hinsley W, Okell LC, van Elsland S, Thompson H, Verity R, Volz E, Wang H, Wang Y, Walker PGT, Walters C, Winskill P, Whittaker C, Donnelly CA, Riley S, Ghani AC (2020) Report 9: Impact of non-pharmaceutical interventions (NPIs) to reduce COVID-19 mortality and healthcare demand. <https://doi.org/10.25561/77482>
- Fraser C, Riley S, Anderson RM, Ferguson NM (2004) Factors that make an infectious disease outbreak controllable. *Proc Natl Acad Sci* 101:6146–6151. <https://doi.org/10.1073/pnas.0307506101>
- Gevertz JL, Greene JM, Sanchez-Tapia CH, Sontag ED (2021) A novel COVID-19 epidemiological model with explicit susceptible and asymptomatic isolation compartments reveals unexpected consequences of timing social distancing. *J Theor Biol* 510:110539. <https://doi.org/10.1016/j.jtbi.2020.110539>
- Giordano G, Blanchini F, Bruno R, Colaneri P, Filippo AD, Matteo AD, Colaneri M (2020) Modelling the COVID-19 epidemic and implementation of population-wide interventions in Italy. *Nat Med* 26:855–860. <https://doi.org/10.1038/s41591-020-0883-7>
- He J, Guo Y, Mao R, Zhang J (2020) Proportion of asymptomatic coronavirus disease 2019 (COVID-19): a systematic review and meta-analysis. *Journal of Medical Virology* <https://doi.org/10.1002/jmv.26326>
- He X, Lau EHY, Wu P, Deng X, Wang J, Hao X, Lau YC, Wong JY, Guan Y, Tan X, Mo X, Chen Y, Liao B, Chen W, Hu F, Zhang Q, Zhong M, Wu Y, Zhao L, Zhang F, Cowling BJ, Li F, Leung GM (2020) Temporal dynamics in viral shedding and transmissibility of COVID-19. *Nat Med* 26:672–675. <https://doi.org/10.1038/s41591-020-0869-5>
- Hellewell J, Abbott S, Gimma A, Bosse NI, Jarvis CI, Russell TW, Munday JD, Kucharski AJ, Edmunds WJ, Sun F, Flasche S, Quilty BJ, Davies N, Liu Y, Clifford S, Klepac P, Jit M, Diamond C, Gibbs H, van Zandvoort K, Funk S, Eggo RM (2020) Feasibility of controlling COVID-19 outbreaks by isolation of cases and contacts. *Lancet Glob Health* 8:e488–e496. [https://doi.org/10.1016/S2214-109X\(20\)30074-7](https://doi.org/10.1016/S2214-109X(20)30074-7)
- Hsiang S, Allen D, Annan-Phan S, Bell K, Bolliger I, Chong T, Druckenmiller H, Huang LY, Hultgren A, Krasovich E, Lau P, Lee J, Rolf E, Tseng J, Wu J (2020) The effect of large-scale anti-contagion policies on the COVID-19 pandemic. *Nature* 584:262–267. <https://doi.org/10.1038/s41586-020-2404-8>
- Johansson MA, Quandelacy TM, K S, Prasad PV, Steele M, Brooks JT, Slayton RB, Biggerstaff M, Butler JC (2021) SARS-CoV-2 transmission from people without COVID-19 symptoms. *JAMA Netw Open* 4(1):e2035057. <https://doi.org/10.1001/jamanetworkopen.2020.35057>
- Kantner M, Koprucki T (2020) Beyond just “flattening the curve”: Optimal control of epidemics with purely non-pharmaceutical interventions. *J Math Ind* 10:1–23. <https://doi.org/10.1186/s13362-020-00091-3>
- Karako K, Song P, Tang W, Kokudo N (2021) Overview of the characteristics of and responses to the three waves of COVID-19 in Japan during 2020–2021. *Biosci Trends* 15(1):1–8. <https://doi.org/10.5582/bst.2021.01019>
- Kuniya T (2020) Prediction of the epidemic peak of coronavirus disease in Japan. *J Clin Med* 9:789. <https://doi.org/10.3390/jcm9030789>
- Kuniya T, Inaba H (2020) Possible effects of mixed prevention strategy for COVID-19 epidemic: massive testing, quarantine and social distancing. *AIMS Public Health* 7(3):490–503. <https://doi.org/10.3934/publichealth.2020040>

30. Lasaulce S, Varma V, Morarescu C, Lin S (2020) How efficient are the lockdown measures taken for mitigating the Covid-19 epidemic? medRxiv. <https://doi.org/10.1101/2020.06.02.20120089>
31. Lauer SA, Grantz KH, Bi Q, Jones FK, Zheng Q, Meredith HR, Azman AS, Reich NG, Lessler J (2020) The incubation period of coronavirus disease 2019 (COVID-19) from publicly reported confirmed cases: Estimation and application. *Annals of Internal Medicine*. <https://doi.org/10.7326/M20-0504>
32. Liu Y, Gayle AA, Wilder-Smith A, Rocklöv J (2020) The reproductive number of COVID-19 is higher compared to SARS coronavirus. *Journal of Travel Medicine*. <https://doi.org/10.1093/jtm/taaa021>
33. Loewenthal G, Abadi S, Avram O, Halabi K, Ecker N, Nagar N, Mayrose I, Pupko T (2020) COVID-19 pandemic-related lockdown: response time is more important than its strictness. *EMBO Mol Med* 12:e13171. <https://doi.org/10.15252/emmm.202013171>
34. Ministry of Health, Labor, and Welfare (2020a). <https://www.mhlw.go.jp/content/3CS.pdf>. Accessed 13 Sept 2022
35. Ministry of Health, Labor, and Welfare (2020b). <https://www.mhlw.go.jp/content/000640250.pdf> Accessed 13 Sept 2022
36. Ministry of Health, Labor, and Welfare (2021a). [https://www.mhlw.go.jp/stf/covid-19/open-data\\_english.html](https://www.mhlw.go.jp/stf/covid-19/open-data_english.html). Accessed 13 Sept 2022
37. Ministry of Health, Labor, and Welfare (2021b). [https://www.mhlw.go.jp/stf/seisakunitsuite/newpage\\_00023.html](https://www.mhlw.go.jp/stf/seisakunitsuite/newpage_00023.html). Accessed 13 Sept 2022
38. Ministry of Land, Infrastructure, Transport and Tourism (2020) [https://corona.go.jp/toppage/pdf/area-transition/20201030\\_stati\\_on.pdf](https://corona.go.jp/toppage/pdf/area-transition/20201030_stati_on.pdf). Accessed 13 Sept 2020
39. Nakajo K, Nishiura H (2021) Transmissibility of asymptomatic COVID-19: Data from Japanese clusters. *Int J Infect Dis* 105:236–238. <https://doi.org/10.1016/j.ijid.2021.02.065>
40. Nakamoto I, Zhang J (2021) Modeling the underestimation of COVID-19 infection. *Results in Physics* 25:104271. <https://doi.org/10.1016/j.rinp.2021.104271>
41. Nakanishi M, Shibasaki R, Yamasaki S, Miyazawa S, Usami S, Nishiura H, Nishida A (2021) On-site Dining in Tokyo During the COVID-19 Pandemic: Time Series Analysis Using Mobile Phone Location Data. *JMIR Mhealth and Uhealth* 9. <https://doi.org/10.2196/27342>
42. Nishiura H, Kobayashi T, Miyama T, Suzuki A, Jung S, Hayashi K, Kinoshita R, Yang Y, Yuan B, Akhmetzhanov AR, Linton NM (2020) Estimation of the asymptomatic ratio of novel coronavirus infections (COVID-19). *Int J Infect Dis* 94:154–155. <https://doi.org/10.1016/j.ijid.2020.03.020>
43. Nishiura H, Linton NM, Akhmetzhanov AR (2020) Serial interval of novel coronavirus (COVID-19) infections. *Int J Infect Dis* 93:284–286. <https://doi.org/10.1016/j.ijid.2020.02.060>
44. Nishiura H, Oshitani H, Kobayashi T, Saito T, Sunagawa T, Matsui T, Wakita T, MHLW COVID-19 Response Team, Suzuki M (2020) Closed environments facilitate secondary transmission of coronavirus disease 2019 (COVID-19). medRxiv <https://doi.org/10.1101/2020.02.28.20029272>
45. Oran DP, Topol EJ (2020) Prevalence of asymptomatic SARS-CoV-2 infection: A narrative review. *Annals of Internal Medicine*. <https://doi.org/10.7326/M20-3012>
46. Our World in Data (2021). <https://ourworldindata.org/grapher/covid-vaccination-doses-per-capita>. Accessed 13 Sept 2022
47. Pachetti M, Marini B, Giudici F, Benedetti F, Angeletti S, Ciccozzi M, Masciovecchio C, C, R, I, D, Z (2020) Impact of lockdown on Covid-19 case fatality rate and viral mutations spread in 7 countries in Europe and North America. *J Transl Med* 18:1–7. <https://doi.org/10.1186/s12967-020-02501-x>
48. Paltiel AD, Zheng A, Sax PE (2021) Clinical and economic effects of widespread rapid testing to decrease SARS-CoV-2 transmission. *Annals of Internal Medicine*. <https://doi.org/10.7326/M21-0510>
49. Pan Y, Darzi A, Kabiri A, Zhao G, Luo W, Xiong C, Zhang L (2020) Quantifying human mobility behaviour changes during the COVID-19 outbreak in the United States. *Sci Rep* 10:1–9. <https://doi.org/10.1038/s41598-020-77751-2>
50. Pataro IML, Oliveira JF, Morato MM, Amad AAS, Ramos PIP, Pereira FAC, Silva MS, Jorge DCP, Andrade RFS, Barreto ML, da Costa MA (2021) A control framework to optimize public health policies in the course of the COVID-19 pandemic. *Scie Rep* 11:1–13. <https://doi.org/10.1038/s41598-021-92636-8>
51. Peirlinck M, Linka K, Costabal FS, Kuhl E (2020) Outbreak dynamics of COVID-19 in China and the United States. *Biomech Model Mechanobiol* 19:2179–2193. <https://doi.org/10.1007/s10237-020-01332-5>
52. Perkins TA, Cavany SM, Moore SM, Oidtmann RJ, Lerch A, Poterek M (2020) Estimating unobserved SARS-CoV-2 infections in the United States. *Proc Natl Acad Sci* 117:22597–22602. <https://doi.org/10.1073/pnas.2005476117>
53. Rahman B, Sadraddin E, Porreca A (2020) The basic reproduction number of SARS-CoV-2 in Wuhan is about to die out, how about the rest of the World? *Rev Med Virol* 30:e2111. <https://doi.org/10.1002/rmv.2111>
54. Senapati A, Rana S, Das T, Chattopadhyay J (2021) Impact of intervention on the spread of COVID-19 in India: A model based study. *J Theor Biol* 523:110711. <https://doi.org/10.1016/j.jtbi.2021.110711>
55. Statistics Division, Bureau of General Affairs, Tokyo Metropolitan Government (2020) <https://www.toukei.metro.tokyo.lg.jp/tenkan/2019/tm19q3e002.htm>. Accessed 13 Sept 2022
56. Sugishita Y, Kurita J, Sugawara T, Yasushi Ohkusa Y (2020) Preliminary evaluation of voluntary event cancellation as a countermeasure against the COVID-19 outbreak in Japan as of 11 March, 2020. medRxiv <https://doi.org/10.1101/2020.03.12.20035220>
57. Tanaka H, Hirayama A, Nagai H, Shirai C, Takahashi Y, Shinomiya H, Taniguchi C, Ogata T (2021) Increased transmissibility of the SARS-CoV-2 alpha variant in a Japanese population. *Int J Environ Res Public Health* 18:7752. <https://doi.org/10.3390/ijerph18157752>
58. Thunström L, Newbold SC, Finnoff D, Ashworth D, Shogren JF (2020) The benefits and costs of using social distancing to flatten the curve for COVID-19. *J Benefit Cost Anal* 11:179–195. <https://doi.org/10.1017/bca.2020.12>
59. Tokyo Metropolitan Government (2020). <https://stopcovid19.metro.tokyo.lg.jp/en/>. Accessed 13 Sept 2022
60. Tokyo Metropolitan Government (2021a). <https://stopcovid19.metro.tokyo.lg.jp/en/cards/deaths-by-death-date>. Accessed 13 Sept 2022
61. Tokyo Metropolitan Government (2021b). [https://www.zaimu.metro.tokyo.lg.jp/syukei1/zaisei/20210129\\_reiwa3nendo\\_tokyo\\_toyosanangaiyou/3yosanangaiyou.pdf](https://www.zaimu.metro.tokyo.lg.jp/syukei1/zaisei/20210129_reiwa3nendo_tokyo_toyosanangaiyou/3yosanangaiyou.pdf). Accessed 13 Sept 2022
62. Tsay C, Lejarza F, Stadtherr MA, Baldea M (2020) Modeling, state estimation, and optimal control for the US COVID-19 outbreak. *Sci Rep* 10:1–12. <https://doi.org/10.1038/s41598-020-67459-8>
63. Tuite AR, Ng V, Rees E, Fisman D (2020) Estimation of COVID-19 outbreak size in Italy. *Lancet Infect Dis* 20:537. [https://doi.org/10.1016/S1473-3099\(20\)30227-9](https://doi.org/10.1016/S1473-3099(20)30227-9)
64. Verity R, Okell LC, Dorigatti I, Winskill P, Whittaker C, Imai N, Cuomo-Dannenburg G, Thompson H, Walker PGT, Fu H, Dighe A, Griffin JT, Baguelin M, Bhatia S, Boonyasiri A, Cori A, Cucunubá Z, FitzJohn R, Gaythorpe K, Green W, Hamlet A, Hinsley W, Laydon D, Nedjati-Gilani G, Riley S, van Elsland S, Volz E, Wang H, Wang Y, Xi X, Donnelly CA, Ghani AC, Ferguson NM (2020) Estimates of the severity of coronavirus disease 2019: a model-based analysis. *Lancet Infect Diseases* 20:669–677. [https://doi.org/10.1016/S1473-3099\(20\)30243-7](https://doi.org/10.1016/S1473-3099(20)30243-7)
65. Wood RM, McWilliams CJ, Thomas MJ, Bourdeaux CP, Vasiliak S (2020) COVID-19 scenario modelling for the mitigation of capacity-dependent deaths in intensive care. *Health Care Manag Sci* 23:315–324. <https://doi.org/10.1007/s10729-020-09511-7>

Springer Nature or its licensor holds exclusive rights to this article under a publishing agreement with the author(s) or other rightsholder(s); author self-archiving of the accepted manuscript version of this article is solely governed by the terms of such publishing agreement and applicable law.